A review of the modeling approaches of the lightning M-component with special attention to their current and electric field characteristics

A Review of Modeling Approaches of the Lightning M-components with Special Attention to their Current and Electric Field Characteristics

Quanxin Li[1,2], Mohammad Azadifar[3,4] , Marcos Rubinstein[3], Farhad Rachidi[4] , Carlo Alberto Nucci[5], Jianguo Wang[2], Jinliang He[1]

[1] State Key Laboratory of Power System, Department of Electrical Engineering, Tsinghua University, Beijing 100084, China
[2] School of Electrical Engineering and Automation, Wuhan University, Wuhan 430072, China
[3] University of Applied Sciences of Western Switzerland (HES-SO), 1400 Yverdon-les-Bains, Switzerland
[4] Electromagnetic Compatibility Laboratory, Swiss Federal Institute of Technology (EPFL), 1015 Lausanne, Switzerland
[5] Department of Electrical and Information Engineering, School of Engineering, University of Bologna, Italy

Abstract—In this paper, we present the characteristics of current, electric fields and modeling approaches of lightning M-component mode of charge transfer. We consider both the classical M-components (occurring after return strokes) and M-component-type ICC (Initial Continuous Current) pulses occurring during the initial (ICC) phase of upward flashes. M-component-type ICC pulses can be distinguished from mixed-mode pulses using different criteria: (i) the 10-90% current risetime at the channel-base with respect to an 8-μs risetime; (ii) the time lag between the onset of the current and electric fields with a respect to a threshold of 10 μs; (iii) an asymmetrical waveform coefficient (AsWc) with respect to a value of 0.8; (iv) the relative height of the junction or connection points on the grounded channel above the ground. The features of M-component electric field waveforms are summarized for close, intermediate, and far distance ranges. The observed millisecond-scale slow-part pulse shows a polarity reversal from an initial-negative waveform at close range, to a full positive-flattening late-time response at intermediate range and a bipolar wave-shape at the far distance range. One or some microsecond-scale fast pulses (junction pulse) are observed to precede the millisecond-scale slow part pulse at intermediate and far distance ranges. The microsecond-scale fast pulses are dominated by unipolar pulses along with several cases of bipolar pulses exhibiting initial polarities of both signs. The main advantage of the guided wave model and its variations is their simplicity and straightforward implementation. The guided wave model is also able to reproduce reasonably well the observed slow electric fields. The nonlinear models are more physics-based compared to the guided wave models. They are based on an important number of adjustable parameters, many of which cannot be directly inferred from experimental observations. The significance of M-components is reviewed according to practical aspects in transformer secondary, surge protective devices (SPD), grounding systems.

***Index Terms*—**: M-component; M-component-type ICC pulses; Modeling Approaches; Electric Field; Current; M-component Mode of Charge Transfer

1. Introduction

M-components are characterized by transient pulses superimposed on the relatively steady continuing current and the associated channel luminosity (e.g., [1]-[3]). M-component-type pulses are also common during the initial stage (Initial Continuous Current – ICC) in upward flashes (e.g., [4]). They are referred to as M-component-type ICC pulses. Experimental data on M-components are available from natural lightning, instrumented towers and triggered lightning. M-components are more numerous than dart leader/return strokes sequences ([5]). Further, M-components have noticeable differences with return strokes in terms of their current peak and rise-time (e.g., [6]-[15]). Despite that, M-components can have significant effects on power networks: they can result in comparable current magnitude to return strokes in the transformer secondary in power systems (*Uman et al.* [16]) and even greater surge energy on the surge protective device (SPD) (*Chen et al.* [17]), and noticeable high voltages on the remote grounding system (*Guo et al.* [18]).

Contrary to return strokes for which the electric fields at various distances are well described (e.g., [19]-[20]), the features of electric fields from M-components are not well documented. Electric field measurements of M-component pulses have been reported at close distance ranges (e.g., 5 m~550 m, [15], [21]-[23]) and intermediate distance ranges (e.g., 2.5 km ~ 27 km, [25]-[29]). The radiated electric fields of M-components were also measured at far distances: 45 km (in [21] and [30]), 79 km and 109 km (in [31] and [32]), and in the range of 68 km to 126 km (in [33]-[34]). The influence of the instrumental decay time on the lightning electric field waveforms was presented in [35].

The first engineering model (classical guided-wave) of M-components consisting of a downward and reflected-and-upward wave was proposed in *Rakov et al.* [36] and it was discussed by *Wang et al.* [37] and *Jiang et al.* [38]. Based on the measurement of currents and electric fields at the Säntis Tower, *Azadifar et al.* [28] proposed a new M-component model that allows to reproduce both the millisecond-scale slow pulse and the preceding microsecond-scale fast pulse. A modification to the classical guided-wave model was proposed in *Li et al.* [34] by assuming an exponential current decay along the grounded channel. In addition, the classical guided-wave model was extended to take into account the presence of an elevated tall object by *Li et al.* [43]-[44]. Non-linear M-component models were proposed in [49]-[51]. The two-wave theory of M-components has found support in experimental observations from VHF interferometers in rocket-triggered lightning (e.g., *Shao et al.* [59] and *Yoshida et al.*[60]) and optical observations through high-speed camera in instrumented towers in *Jiang et al.*[61].

In this study, which is an extension of the preliminary study presented in *Li et al.* [45], we summarize the recent progress in M-component modeling and characterization based on the following aspects: 1) current measurement and current pulse classification, 2) electric field features, 3) modeling approaches, and 4) practical aspects. Note that both classical M-components and M-component-type ICC pulses are considered in the present study. The organization of the paper is as follows. A summary of the current measurements and electric field measurements associated with M-components is presented respectively in sections 2 and 3. Section 4 is devoted to modeling approaches of the M-component mode of charge transfer. Practical aspects related to M-components are discussed in Section 5. Discussion and summary are given in the final section.

2. Summary of the Current Measurement of M-component

2.1 Current parameters

Fisher et al. [6] analyzed lightning currents of return strokes and the overall continuing current measured associated with rocket-triggered lightning events in Florida and Alabama. Later, the data associated with M-components were analyzed in *Thottappillil et al.* [5]. They reported that a typical M component is characterized by a more or less symmetrical current pulse having (1) an amplitude of about 100 to 200 A (about 2 orders of magnitude lower than that for a return stroke, (2) a risetime of 300 to 500 μs (3 orders of magnitude longer than that for a return stroke, and (3) a charge transfer to ground of the order of 0.1 to 0.2 C (1 order of magnitude smaller than that for a subsequent return stroke pulse).

Qie et al. [15] discussed data associated with 18 typical M components and 5 large M components with unusual large peak current in the range of kiloamperes. For typical M components, the geometric mean of the peak current, the half peak width, and the 10-90% risetime were respectively 243 A, 400 μs, and 319 μs. For the large M components, the corresponding values were respectively 5.1 kA, 76.3 μs, and 34.6 μs. They reported a return-stroke-M-component (RM) event which implies a superposition of the dart leader and the M-component incident wave in the channel. The event was ascribed as a simultaneous coexistence of two branches in the upper part of the discharge channel with a common lower portion.

Based on records of current and electric field observations at Morro do Cachimbo Station, *Visacro et al.* [10] reported that the frequency of first return strokes exhibiting M components is within the range of tens of percent instead of a few percent. They found that most of the analyzed first-return-stroke M-components of natural lightning occur at the final phase of the

return-stroke process and not during the flow of continuing currents. Apparently, this also holds true for most of the first M-components of subsequent return strokes.

Zhang et al. [58] reported that the geometric average values of peak current, duration, 10–90% risetime, half peak width, and charge transfer from the beginning to the end are respectively 185.75 A, 1.68 ms, 0.42 ms, 0.70 ms and 0.11 C. As for the CC, the duration, average current and charge transfer are respectively 19.01 ms, 202.58 A and 3.85 C. They also reported that the existence of M-components with small mean amplitude (<0.5 kA) is a necessary condition for long CCs. In *Zhang et al.* [63], the current characteristics of 239 M-components in 18 triggered lightning flashes are analyzed. Sixty-eight of the events (28%) had peak currents exceeding 1 kA. The geometric average values of the peak current, duration, 10–90% risetime, half peak width, charge transfer, interval from return stroke to M-component and background current amplitude are 2.358 kA, 0.627 ms, 0.078 ms, 0.165 ms, 0.417 C, 2.172 ms, and 579 A, respectively. The M events with large peak currents and steepnesses occurred closer in time to the preceding return stroke.

Li et al. [43] proposed two different waveforms for the M-component wave in their analysis, a fast and a slow current, represented using Heidler's function, as shown in Fig. 1. The current magnitude was set to 1 kA. The asymmetrical waveform coefficients (AsWC) for the two waveforms are, respectively, 0.79 and 0.58, satisfying the criterion for an M-component mode of charge transfer (*He et al.* [12]). A fully symmetrical pulse is characterized by an AsWC equal to 1/2, while waveforms characteristic of return strokes or mixed-mode pulses have AsWCs close to 1.0. According to *He et al.* [12], if the AsWC for a pulse superimposed on the ICC is lower than 0.8, the pulse is classified as an M-component-type ICC pulse. Furthermore, the 10-90% risetimes are 11.0 μs and 404.0 μs, both satisfying the criterion of *Flache et al.* [14], in which ICC pulses with risetimes higher than 8 μs were ascribed to the M-component type of charge transfer. The risetime of the fast M-component waveform is within the range of measured M-components of rocket-triggered lightning (*Qie et al.* [15]) and of natural negative cloud-to-ground lightning measured in Morro do Cachimbo (*Visacro et al.*, [10]). The 10-90% risetime of the slow waveform agrees well with the data reported by *Thottappillil et al.* [5].

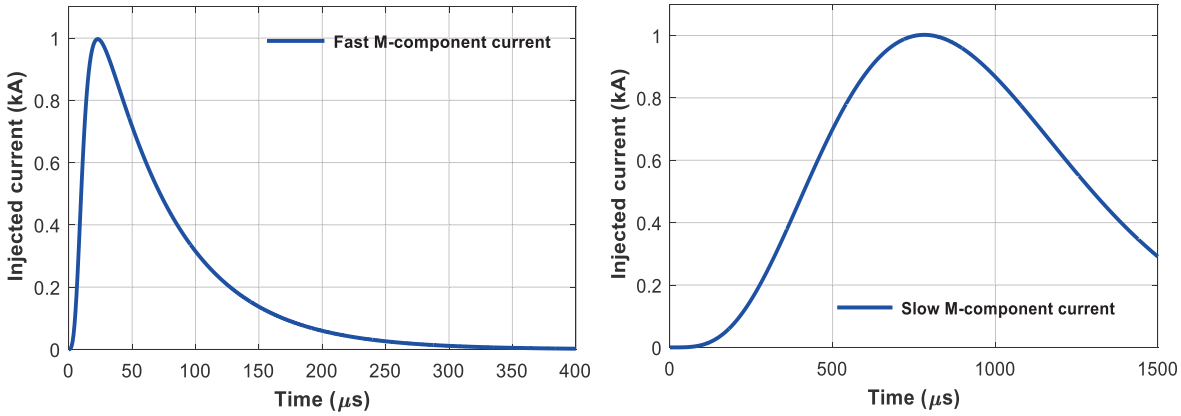

Figure 1. M-component current waveform (a) Fast waveform. (b) Slow waveform. Adapted from *Li et al.* [43]

Table 1. Parameters of the M-component injected current. Adapted from *Li et al.* [43]

	I_1(kA)	$\tau_1(\mu s)$	$\tau_2(\mu s)$	n	10-90% risetime(μs)	AsWc
Fast Waveform	1.02	12	60	3	11.0	0.79
Slow Waveform	0.77	2000	200	4	404.0	0.58

2.2 Classification of lightning M-component mode of charge transfer

The similarity of the initial continuous current pulse (ICCP) and the M-component was first noted by *Wang et al.* [7] through the measured channel-base current in rocket-triggered lightning. According to *Rakov et al.* [21], there are three typical charge transfer modes during negative cloud-to-ground flashes: (1) the dart leader/return stroke mode, (2) the continuing current mode, and (3) the M-component mode of charge transfer. *Miki et al.* [8] compared the characteristics of ICC pulses observed in measurements using instrumented towers in Austria, Germany, and Japan to those in rocket-triggered lightning in Florida. They reported that the former exhibit larger peaks, shorter risetimes, and shorter half-peak widths than the latter. The occurrence of the ICC pulses with short risetimes is assumed to be due to low-altitude upward branches in object-initiated lightning [9].

Based on the observations at Peissenberg Tower in Germany, *Flache et al.* [14] analyzed simultaneous current and high-speed video records for 33 ICC pulses and 9 M-components in 8 upward flashes. They found that both ICC pulses and M-components with longer 10-to-90% risetimes (>8 μs) tended to occur in already luminous channels, and hence were interpreted as indicative of the M-component mode of charge transfer to ground, while those with shorter 10-to-90% risetimes (< 8μs) tended to involve a newly-illuminated, low-altitude branch and, hence, were attributed to the leader/return-stroke mode of charge transfer in that branch.

Based on observations of 31 distinct current pulses in rocket-triggered lightning, *Qie et al.* [15] analyzed simultaneous current and close electric field measurements for ICC pulses, M-

components, and return strokes. They found that the time interval between the impulsive current onset and close electric field peak for the ICC pulse and M-components was typically some tens of microseconds, while it was less than 1 μs for leader/return stroke sequences.

In addition to the three individual modes, the term "mixed mode" of charge transfer was introduced by *Zhou et al.* [22]-**Error! Reference source not found.** to describe the transfer of charge associated with faster pulses superimposed on the initial continuous current (ICC) in upward negative flashes. Using observations from the Gaisberg Tower, the M-component mode of charge transfer was classified into mixed-mode and classical M-component mode through the time lag between the current and fields, the time lag being typically tens of microseconds for the M-component mode and noticeably shorter (< 10μs) for the mixed mode. The mixed-mode indicates a lower excitation (junction) point compared to the classical M-component mode.

Based on simultaneously observed current and electric fields of 44 return-stroke type ICC pulses and 24 return strokes at the Säntis Tower, two different types of ICC pulses were identified in *Azadifar et al.* [27]: (1) M-component-type pulses, for which the electric field pulse occurs significantly earlier than the onset of the current pulse, and (2) fast pulses (return-stroke type ICC pulses), for which the onset of the field matches that of the current pulse. A similarity of the return-stroke type ICC pulses with return strokes was found and they suggested that return-stroke type ICC pulses are associated with the mixed mode of charge transfer to ground.

In He et al. [12], four types of current pulses are observed among a total of 109 pulses: (1) return-stroke pulses; (2) mixed-mode ICC pulses, which have characteristics very similar to those of return strokes and are believed to be associated with the reactivation of a decayed branch or the connection of a newly created channel to the ICC-carrying channel at relatively small junction heights; (3) classical M-component pulses; and (4) M-component-type ICC pulses, presumably associated with the reactivation of a decayed branch or the connection of a newly created channel to the ICC-carrying channel at relatively large junction heights.

In summary, current pulse classifications can be summarized through the following aspects.

(1) 10-90% risetime of the channel-base current waveform: mixed mode pulses if the risetime is lower than 8 μs and M-component mode pulses if larger.

(2) Time lag between the onset of the current and electric fields: mixed mode pulses if the lag is shorter than 10 μs, and M-component mode pulses if larger.

(3) Asymmetrical waveform coefficient (AsWc): the value is usually larger than 0.8 for return strokes and mixed mode ICC pulses, while it is usually smaller than 0.8 for M-component mode pulses.

(4) The relative height of the junction or connection points on the grounded channel above the ground. Large junction heights (>1 km) correspond to M-component mode pulses, while smaller heights correspond to mixed mode pulses.

Recently, *Watanabe et al.* [67] analyzed 58 upward flashes initiated from the Gaisberg Tower in Austria during 2006-2014. Forty-six flashes (79%) were characterized by a negative continuous current (CC), and 12 flashes (21%) by a bipolar CC. There were 1180 current pulses that occurred during the initial stage (IS) of these 58 flashes, of which 708 (60%) were bipolar with an initial positive excursion, 28 (2.4%) were positive unipolar, 440 (37%) were negative unipolar, and four (0.3%) were bipolar with an initial negative excursion. They found that bipolar current pulses only occurred in the IS at early times. The ICC was divided into two phases: (1) upward leader initiation and propagation phase (IPP), and (2) upward leader mature phase (MP). Nine hundred and one or 76% of the pulses occurred during the IPP, and 279 or 21% of the pulses occurred during the MP.

3. Summary of the Observed Features of Electric Fields Associated with M-components

The electric fields from the M-components often includes one or a few microsecond-scale fast pulses preceding the millisecond-scale slow-part pulse. Experimental observations from different studies reveal that the features of microsecond-scale and millisecond-scale pulses would change at different distances. In what follows, we summarize features of these pulses at close, intermediate, and far distance ranges. Note that the electric fields presented in the present paper follow the atmospheric electricity sign convention, unless otherwise specified.

3.1. Close Distance (5 m~550 m)

Based on electric field measurements associated with triggered-lightning experiments at the ICLRT at Camp Blanding, Florida [21], a total of 16 M-components were recorded in 1997, 1999 and 2000. The observation distances ranged from 5 m to 557 m. Among the observed data, the electric field at 5 m shows a positive polarity overshoot in the second half-cycle (see Figure 2b). According to the data in *Rakov et al.* [21], except the one at 5 m, the observed M-component electric field typically shows a unipolar-negative pulse.

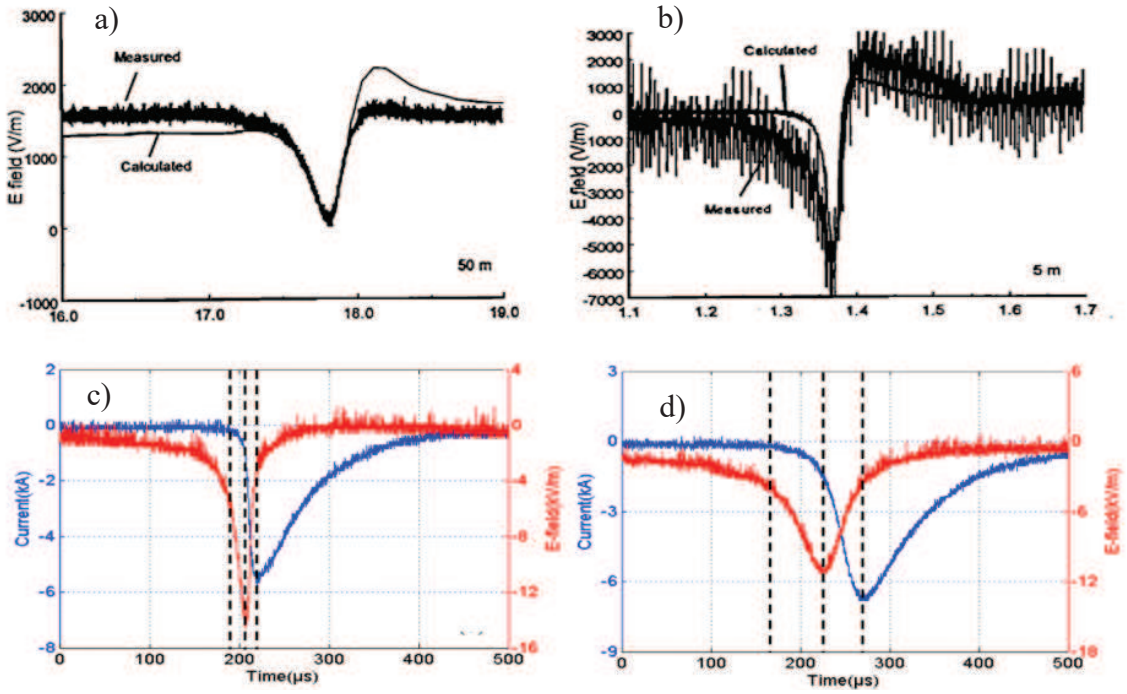

Figure 2. The observed M-component electric fields from rocket-triggered lightning by *Rakov et al.* [21] (a, b) and *Qie et al.* [15] (c, d).

Qie et al. [15] made simultaneous measurements of 18 typical M-components, 5 large amplitude M-components, 3 ICC pulses, and 1 so-called stroke–M-component (RM) event. The RM event was a superposition of a dart leader and an M-component incident wave in two branches with a common lower portion coexisting simultaneously in the upper part of the channel. The electric field was measured at 30 m from the channel. It was shown that (see Figure 2c and d) the electric fields from M-components, ICCP and RM were all unipolar negative pulses.

Zhou et al. **Error! Reference source not found.** obtained current and associated electric fields at the Gaisberg Tower, Austria. The electric fields were measured at a distance of 170 m from the tower. According to the 2 ICC pulses and 4 M-components shown in *Zhou et al.* **Error! Reference source not found.**, the electric fields of ICC pulses were bipolar with an initial-negative polarity followed by a positive overshoot, while the M-component electric fields were characterized by negative bipolar waveforms (see Figure 3). Note that the ICC pulses mentioned in *Qie et al.* [15] are M-component like pulses, while *Zhou et al.* **Error! Reference source not found.** presents both M-component-type ICC pulses and mixed mode pulses (*He et al*. [12].

Three hundred and forty field waveforms measured at Gaisberg Tower at 170 m were analyzed by *Watanabe et al.* [68]. 68 (20%) were associated with current pulses occurring

during the initiation and propagation phase (IPP) of the upward leader, and 272 (80%) were associated with pulses that occurred during the mature phase (MP) of the upward leader. Of the 68 field waveforms, 40 were associated with bipolar (IPP-B type) current pulses and 28 were associated with unipolar (IPP-U type) current pulses. Field signatures of IPP-B pulses were only detected at the near measurement station and appear to be associated with currents in relatively short (meter-scale) channel segments formed during the upward leader inception.

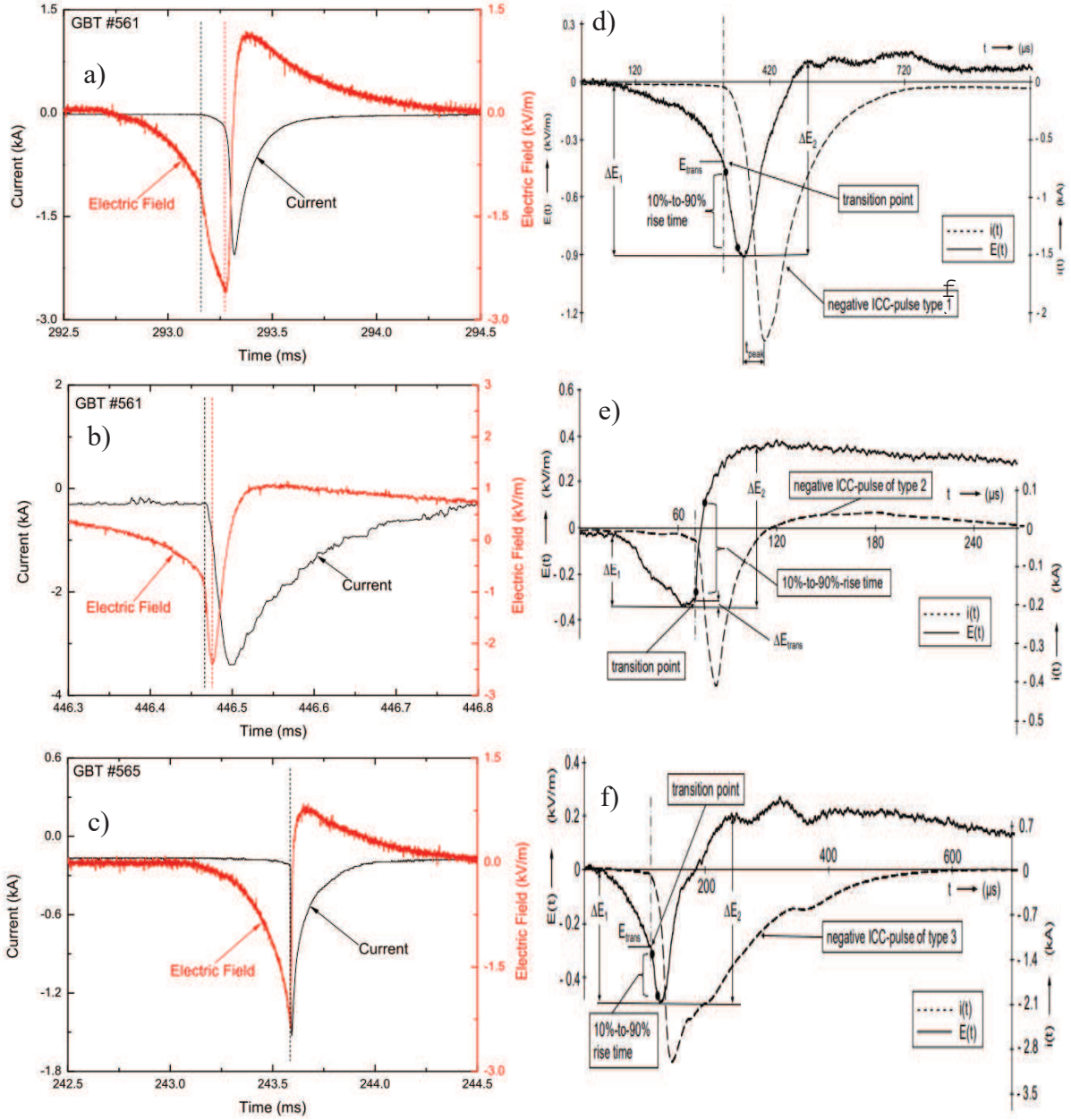

Figure 3. The observed electric fields from rocket-triggered lightning by *Zhou et al.* **Error! Reference source not found.** (a, b, c) and *Paul and Heidler* [23] (d, e, f).

At the Peissenberg Tower, *Paul and Heidler* [23] obtained currents and associated electric fields 180 m from the tower. The data comprise 108 ICC-pulses and 26 M-components in 17 negative lightning flashes. Based on the observed current waveforms, the time-synchronized

electric fields are classified into three types: 71 current pulses with a symmetrical wave shape (type I), 12 current pulses with a bipolar waveform (type II), and 6 current pulses with a fast rise and long decay (type III) (see Figure 3d, e, and f). The electric fields exhibited a positive overshoot at the late-time response that lasted hundreds of microseconds.

In summary, the main features of the field waveforms at this distance range are:

(1) The electric field (millisecond-scale slow part pulse) can be categorized into two types of pulses: (i) a salient unipolar pulse with an initial-negative polarity [15],[21] and [34], (ii) a bipolar pulse with initial-negative polarity followed by a positive excursion of the late-time response ([4],[23] and one case in *Rakov et al.*[21]);

(2) The pulse width is hundreds of microseconds and the magnitude is in the order of kV/m;

(3) The microsecond-scale fast pulses have never been observed in this range of distances.

3.2. Intermediate Distance (2 km~27 km)

Rakov et al. [26] analyzed the electric fields of microsecond-scale fast pulses from two datasets (Tampa (27 CG flashes measured at distances of 2.5 km to 12 km) and Kennedy Space Center-KSC (19 CG flashes measured at distances of 5 km to 27 km)). Microsecond-scale fast pulses were seen in 44% (39 out of 88) of the M-components in flashes measured in Tampa and in 77% (23 out of 30) of the M-components in flashes measured at KSC. The observed microsecond-scale fast pulses (electric fields) of M-components were classified into five groups, namely unipolar and bipolar pulses with an initial negative and positive polarity as well as irregular ones. The pulses belonging to the first four groups are illustrated in Figure 4.

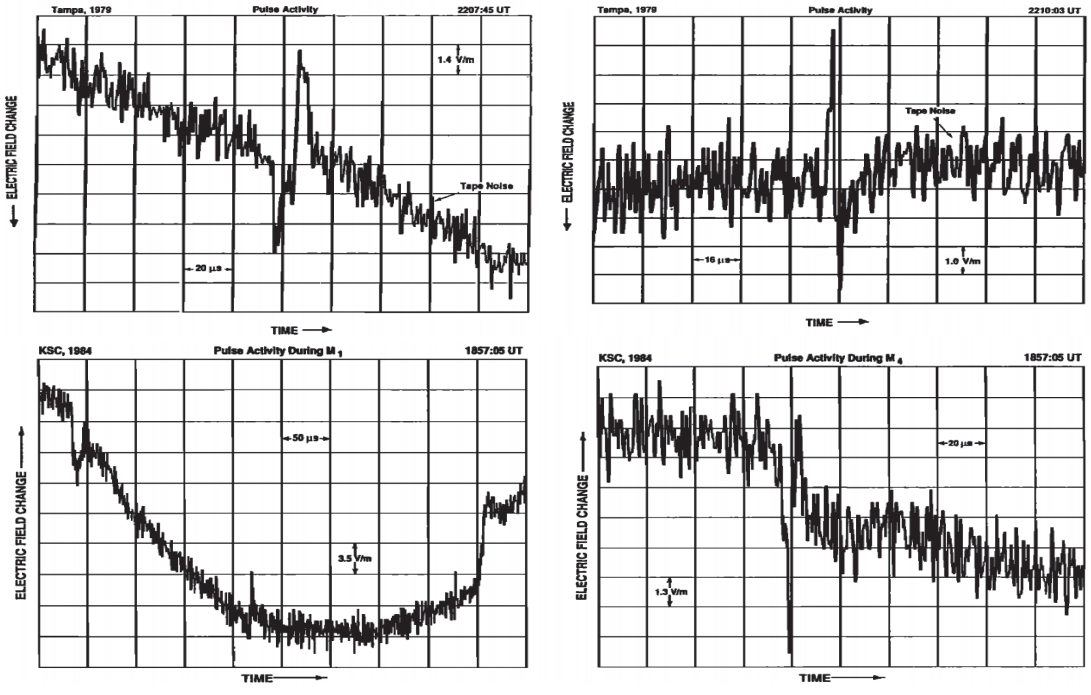

Figure 4. The observed electric fields (fast pulses) from *Rakov et al.* [26].

Azadifar et al. [27] presented time-synchronized measurements of current and electric fields at 14.7 km associated with upward flashes at the Säntis Tower in Switzerland. A total of 9 flashes consisting of 44 RS-type ICC pulses and one M-component-type ICC pulse were analyzed. As shown in Figure 5a, the microsecond-scale fast pulse of M-component-type pulses precedes the onset of the current by tens of microseconds. The millisecond-scale slow-part pulse is also seen (Figure 5b). In addition, 11 out of 13 of the so-called microsecond-scale fast pulses were reported as unipolar pulses in *Azadifar et al.* [28] and the remaining were bipolar pulses with an initial-positive polarity.

An analysis of current and electric field waveforms obtained at the Säntis Tower was carried out by *He et al.* [12]. Their data contained 100 pulses, of which 70 mixed-mode ICC pulses, 11 classical M-component pulses, and 19 M-component-type ICC pulses. Forty-one percent (29 out of 70) of the electric fields associated with mixed-mode ICC pulses were preceded by microsecond-scale fast pulses occurring some hundreds of microseconds prior to the onset of the current. The electric fields from classical M-component pulses were characterized by an initial rising part that levels off after the peak at a value greater than zero at the late-time and they lasted one or more milliseconds (see the bottom right panel in Fig.5).

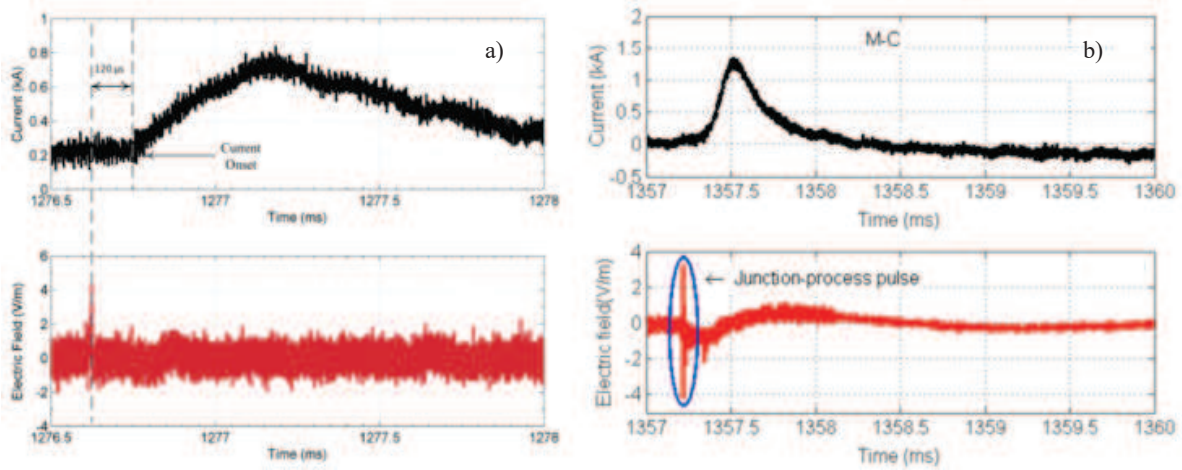

Figure 5. The observed electric fields from the Säntis Tower by *Azadifar et al.* [27] (a) and *He et al.* [12] (b).

In summary, the main features of the field waveforms at this distance range are:

(1) The millisecond-scale slow part pulse (15 km) from a classical M-component pulse is characterized by an initial rising part that levels off after the peak at a value greater than zero at the late-time and they lasted one or more milliseconds ([27], [12]).

(2) Some millisecond-scale slow part pulses are preceded by microsecond-scale fast pulses (41% of 70 mixed-mode ICC pulses in [12]; 44% of 88 (Tampa) and 77% of 30 (KSC) in [26]);

(3) The observed microsecond-scale fast pulses are predominantly positive, unipolar ones; some cases of bipolar pulses with an initial-positive polarity were also reported ([26], [28]). Both polarities are reported in *Rakov et al.* [26].

It is worth noting that the microsecond-scale fast pulse has not been observed in a number of measurements made at close distances (e.g., [15], [21]-[24], [34]). The reason for this is that this pulse is overwhelmed by the fields radiated from the grounded conducting channel due to its closer distance to the field measuring sensor. On the other hand, at far distances (50 km and beyond), the fast pulse becomes dominant and it is the slow, millisecond pulse that is generally not discernible. *Azadifar et al.* provide an interesting theoretical analysis of the relative importance of the fast and slow pulses as a function of distance [27].

3.3. Far Distance (45 km~126 km)

Distant electric field (45 km) measurements of M-components were obtained by *Rakov et al.* [21] at ICLRT at Camp Blanding, Florida. The observed microsecond-scale fast pulse exhibits a bipolar wave-shape with an initial positive polarity followed by a negative overshoot (see Figure 5a).

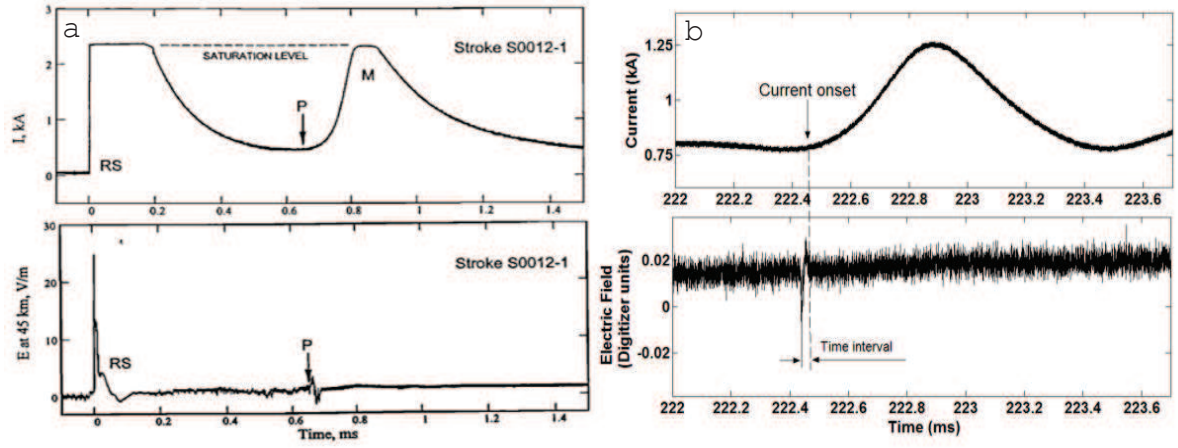

Figure 6. The observed microsecond-scale fast pulses at 45 km by *Rakov et al.* [26] (a) and *Tran et al.* [30] (b).

Similarly, *Tran et al.* [30] analyzed 120 M-components in 11 flashes at ICLRT with electric fields measured at 45 km. They reported that 50% of the 76 pronounced M-component current pulses (with magnitudes larger than 165 A) were preceded by microsecond-scale fast pulses. Out of the 120 M-components, 43 (36%) were preceded by microsecond-scale fast pulses. Note that the relatively low magnitude of the millisecond-scale slow part pulse is not discernible in Figure 6 b. Note that the physics sign convention (opposite to the atmospheric electricity sign convention) was used for the electric field in Figure 6b.

At the Gaisberg Tower, *Pichler et al.* [31] conducted current and associated electromagnetic field observation at two distances (79 km and 109 km). Their data consist of 145 ICC pulses. The observed millisecond-scale slow part pulses showed a bipolar trend with an initial-negative polarity followed by a positive excursion (see Figure 7). The overshoot ratio is about 0.8. The microsecond-scale fast pulse was found to be superimposed on the wavefront of the millisecond-scale slow part pulse.

Vayanganie et al. [32] reported 17 M-components in 14 flashes in Sri Lanka, in which the measured millisecond-scale slow-part pulses featured bipolar waveforms embedded with chaotic fast pulses. Figure 7b shows one of the results in *Vayanganie et al.* [32] where the overshoot ratio is around 0.7. The observed electric field waveform indicates a relatively far observation distance (the precise distance value is not mentioned in the paper). Fourteen M-components followed the first return stroke and 3 followed subsequent returns strokes. The mean time durations for the millisecond-scale slow part pulses are reported as 343 μs and 157 μs, respectively.

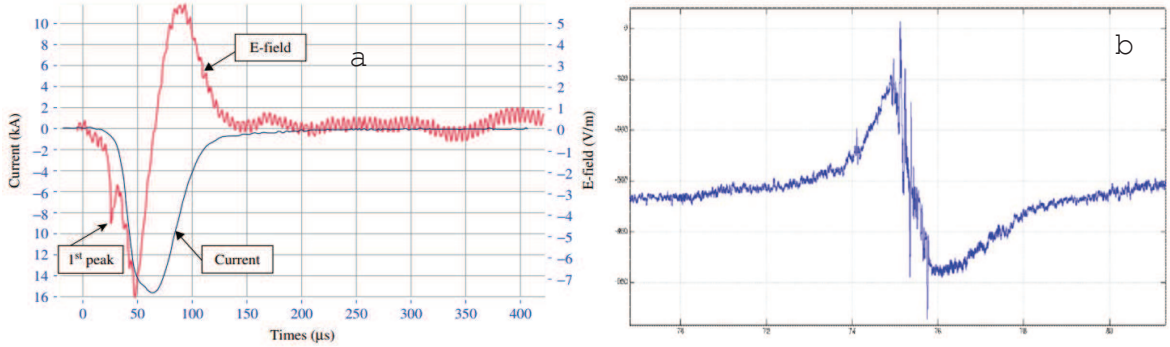

Figure 7. The observed electric fields (slow part pulses) by *Pincher et al.* [31] (a) and *Vayanganie et al.* [32] (b). The sign convention used in the electric field shown in (a) is the physics sign convention. The overall time duration for the slow part pulse in (b) is 2590 μs.

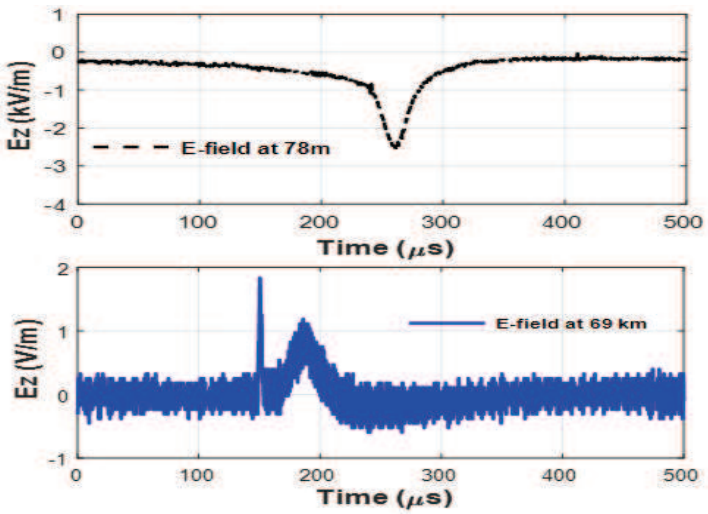

Figure 8. The simultaneously observed close and far electric fields in *Li et al.* [34].

Li et al. [34] analyzed an M-component in a rocket-triggered lightning. Their data include current, field measurement at 78 m, and six far field measurements at distances of 68 to 126 km. The fast microsecond-scale pulse and the ensuing slow millisecond-scale pulse were observed simultaneously (see Figure 8). A zero-crossing of the slow part pulse was observed at all the six far observation points. The overshoot ratio was around 0.3.

In summary, the main features of the field waveforms at this distance range are:

(1) The millisecond-scale slow part pulse is bipolar with an initial positive polarity and a negative overshoot in the second half cycle ([31], [34]);

(2) Some millisecond-scale slow-part pulses are preceded by microsecond-scale fast pulses (36% in *Tran et al.,* [30]);

(3) The observed microsecond-scale fast pulse [26] and millisecond-scale slow-part pulses [32] are embedded with chaotic pulses;

(4) Microsecond-scale fast pulses can be bipolar with negative initial polarity [30], bipolar with positive initial polarity [26], or unipolar with positive polarity [34].

4. Modeling Approaches of the M-component Mode of Charge Transfer

4.1 Guided-wave M-component model of Charge Transfer

a. Rakov et al. [36]

According to this model, the M-component involves a downward-propagating incident wave followed by an upward-propagating reflected wave. Based on this mechanism, *Rakov et al.* [36] proposed the first engineering model for the M-component, in which the M-component current $i(z', t)$ at a given height z' along a straight vertical channel of height L at a time t is expressed as follows:

$$i(z',t) = \begin{cases} i(L, t - \dfrac{L - z'}{v}), & if \;\; t < \dfrac{L}{v} \\ i(L, t - \dfrac{L - z'}{v}) \; + \; i(L, t - \dfrac{L + z'}{v}), & if \;\; t \geq \dfrac{L}{v} \end{cases} \tag{1}$$

where v is the M-wave propagation speed and $i(L, t)$, which is the current injected at the top of the channel, equals half of the total current measured at the channel-base. Each of the two M-component waves is described by the classical transmission line model, and the current reflection coefficient at ground is assumed to be equal to unity. *Rakov et al.* [36] tested the validity of the model using the measured channel-base M-component current, the measured electric field at 30 m from the channel and an adjustable speed of the incident and reflected M-

waves. The model was also used in the modeling of the different charge transfer modes in upward flashes at the Säntis Tower by *He et al.* [39] and a large bipolar event, also at the Säntis Tower, by *Azadifar et al.* [40].

b. Jiang et al. [38]

Jiang et al. [38] presented a modification to the M-component model proposed by *Rakov et al.* [36]. As shown in Figure 9, the modified M-component model involves a downward wave transferring negative charge from the upper to the lower channel and an upward wave draining the charge transported by the downward wave.

Assume t_0 to be the instant at which the downward wave reaches the ground, and v_1 and v_2 the propagating velocity of the downward and upward waves, respectively. At a time t' ($t' > t_0$), the height of the interface of the downward and upward waves is H', where $H' = v_2 (t' - t_0)$. At the same time, the line charge density of the channel beneath H' is zero.

The channel-base current is assumed to be equal to the current at the interface of the upward and downward wave

$$I_{base}(t') = I_{H'}(t') = \rho\left(H', t'\right)(v_1 + v_2) \tag{2}$$

The charge at a height H' (at the time t'), namely $\rho\left(H', t\right)$, lowered from the height h' (at the time t_0) during $t_0 \sim t'$ is given by

$$\rho\left(H', t'\right) = \rho\left(h', t_0\right) \tag{3}$$

$$h' = H' + v_1(t' - t_0) = (v_1 + v_2)(t' - t_0) \tag{4}$$

Combining equations (4) and (3) yields

$$\rho\left((v_1 + v_2)(t - t_0), t_0\right) = I_{base}(t') / (v_1 + v_2) \tag{5}$$

The line charge density $\rho\left(z', t\right)$ at any height of the channel at t_0 can be derived as

$$\rho\left(z', t\right) = \begin{cases} \rho\left(z' + v_1(t - t_0), t_0\right), \\ 0, \qquad\qquad t \geq t_0 \ \& \ z' < v_2(t - t_0) \end{cases} \tag{6}$$

The modified model was tested using simultaneously measured channel-base currents and close electric fields (50 m and 550 m) of one M-component associated with rocket-triggered lightning. The results showed a reasonable agreement between the simulated and the measured electric field waveforms at both distances.

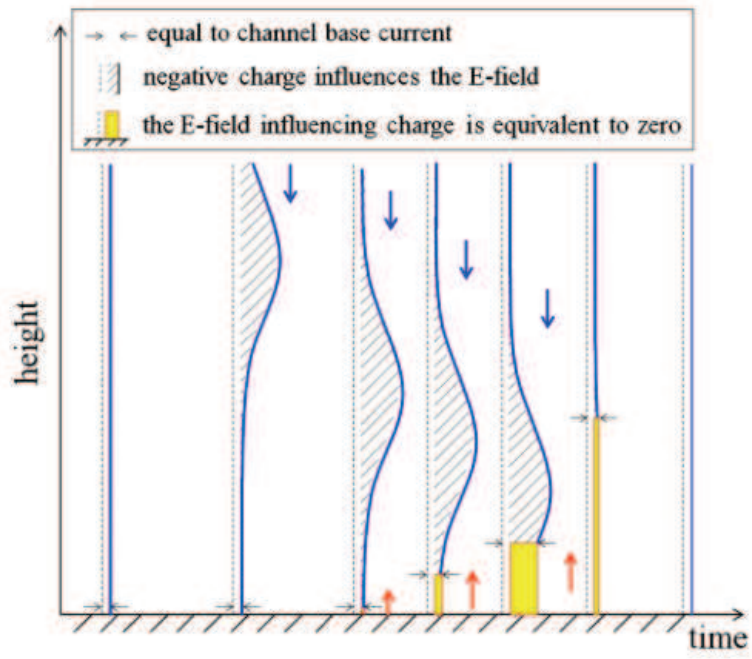

Figure 9. Diagram of the modified mechanism of M-component from *Jiang et al.* [38].

c. Azadifar et al. [28]

The previous models were aimed at simulating only the slow pulse of the M-component electric field. *Azadifar et al.* [28] presented a new engineering model for the M-component mode of charge transfer to ground that can predict the observed electric field signatures associated with M-components at various distances, including (1) the microsecond-scale pulse thought to be due to the junction of in-cloud leaders and the grounded, current-carrying channel, and (2) the ensuing slow, millisecond-scale pulse due to the M-component occurring below the junction point. To model the process that gives rise to the microsecond-scale pulses, they hypothesize that the current pulses propagating away from the junction point along the main lightning channel and along the feeding in-cloud leader channel carry the same amount of charge. The current along the grounded channel was treated using the guided-wave model (*Rakov et al.* [36]), using Equation (1). They further assumed that the pulse traversing the feeding branch is similar to a subsequent return-stroke pulse. In the proposed model, the return-stroke-like process is represented by the modified transmission line model with exponential decay (MTLE) (*Nucci et al.,* [46], *Rachidi and Nucci* [47]). The current distribution along the branch is

$$i_0(r,t) = i_c(t - r/v_0)u(t - r/v_0)e^{-r/\lambda_0} \tag{7}$$

in which i_c(t) is the current at the junction point propagating along the branch, λ_0 is the MTLE

attenuation constant, and v_0 is the propagation velocity. The typical subsequent return-stroke current waveform (i_{typ}(t)) used in [48] was used to specify the shape of i_c(t).

$$i_c(t) = i_{typ}(t) \times q \tag{8}$$

where q is determined using the charge conservation at the junction point during the whole attachment process of the branch and the grounded channel as follows

$$q = \frac{\int_0^\infty i(L,t')dt'}{\int_0^\infty i_{typ}(t')dt'} \tag{9}$$

where $i(L,t')$ is the injected current at the junction point propagating along the grounded channel (see Equation (1)), and i_c(t) can be found using equations (8) and (9).

The proposed model was able to successfully reproduce the vertical electric field waveforms at 14.7 km associated with the M-component processes in upward lightning flashes initiated from the Säntis Tower, in which both the fast microsecond-scale and the following slow millisecond-scale pulses were observed. The model from *Azadifar et al.* [28] was later discussed and modified by adding the current exponential attenuation in *Li et al.* [69].

d. Li et al. [34]

In their study, *Li et al.* [34], based on the observations form *Jordan et al*. [53], *Kotovsky et al.* [54], *Wang et al.* [55], and *Stolzenburg et al.* [62], proposed to use a modified version of the M-component guided-wave theory in which the M-component current waves decay exponentially while traveling along the channel, in a similar way as in the Modified Transmission Line Model with exponential decay (MTLE) for the return stroke (*Nucci et al.* [46], *Rachidi and Nucci* [47]). For the sake of simplicity, the decay constants for the downward and upward waves were assumed to be equal. The distribution of the M-component current along the continuing-current-carrying channel is expressed as follows,

$$i(z',t) = \begin{cases} i(L,t-\dfrac{L-z'}{v})e^{-\frac{L-z'}{\lambda}}, & if \quad t < \dfrac{L}{v} \\ i(L,t-\dfrac{L-z'}{v})e^{-\frac{L-z'}{\lambda}} + i(L,t-\dfrac{L+z'}{v})e^{-\frac{L+z'}{\lambda}}\rho_g, & if \quad t \geq \dfrac{L}{v} \end{cases} \tag{4}$$

where λ is the decay constant of the current.

The electric fields calculated using the model proposed by *Li et al.* [34] were in better agreement, compared to the original model of Rakov et al. [36], with the measurements at both close and distant ranges.

e. Li et al. [43]

Li et al. [43]-[44] proposed an extension of the guided-wave M-component model of *Rakov et al.* [36] considering the presence of a vertically elevated strike object. The proposed extension was motivated by the fact that (1) M-components and ICC pulses occurring in upward flashes initiated by tall towers are usually modelled by neglecting the transient processes along the tower, and (2) the effect of the tower might be of importance in case of very tall structures such as the CN Tower (553 m) in Toronto or the Tokyo Skytree (634 m) in Tokyo, and for M-components with relatively fast risetimes. They followed the procedure used for return strokes by *Rachidi et al.* [41]. The tall object was represented as a lossless, uniform transmission line. They derived the following expressions for the current distribution along the channel and along the strike object

$$\begin{aligned} i(z',t) &= i\left(L, t-\frac{L-z}{v}\right)u\left(t-\frac{L-z}{v}\right) \\ &-\rho_t i\left(L, t-\frac{L+z-2h}{v}\right)u\left(t-\frac{L+z-2h}{v}\right) \\ &+(1-\rho_t)(1+\rho_t)\sum_{n=0}^{\infty}\rho_g^{n+1}\rho_t^{n} i\left(L, t-\frac{L+z-2h}{v}-\frac{2(n+1)h}{c}\right)u\left(t-\frac{L+z-2h}{v}-\frac{2(n+1)h}{c}\right) \end{aligned} \tag{10}$$

$$i(z',t) = (1-\rho_t)\left\{\begin{array}{l} \sum_{n=0}^{\infty}\rho_g^{n+1}\rho_t^{n} i\left(L, t-\frac{L-h}{v}-\frac{h-z}{c}-\frac{2nh}{c}\right)u\left(t-\frac{L-h}{v}-\frac{h-z}{c}-\frac{2nh}{c}\right) \\ +\sum_{n=0}^{\infty}\rho_g^{n+1}\rho_t^{n} i\left(L, t-\frac{L-h}{v}-\frac{h+z}{c}-\frac{2nh}{c}\right)u\left(t-\frac{L-h}{v}-\frac{h+z}{c}-\frac{2nh}{c}\right) \end{array}\right\} \tag{11}$$

where n is an index representing the successive multiple reflections occurring at the two ends of the strike object, v is the M-component wave propagation speed along the channel and h is the height of the tower. The parameters ρ_g and ρ_t are the reflection coefficients at the ground and at the tower top, respectively.

Simulation results for the radiated electric field show that, for very tall structures and fast M-component waves, the presence of a tall strike object can result in a sharp peak superimposed on the M-component electric field. For slow M-component waveforms or for moderately tall structures, the presence of the tall strike object can be disregarded in the M-component field calculations.

4.2 Nonlinear M-component model of Charge Transfer

a. Bazelyan [49]

Bazelyan [49] published a paper about M-component modeling almost simultaneously with the one from *Rakov et al.* [36]. The M-component was treated as a transient process in an RLC distributed circuit. *Bazelyan* [49] interpreted the M-component as representing the discharge, into the earth, of an intercloud leader after its contact with the upper end of a preceding grounded but still conductive channel. The current distribution along the grounded channel and the branch were simulated applying the telegrapher's equations

$$-\frac{\partial u(z',t)}{\partial z'} = L\frac{\partial i(z',t)}{\partial t} + Ri(z',t) \tag{12}$$

$$-\frac{\partial i(z',t)}{\partial z'} = C\frac{\partial u(z',t)}{\partial t} \tag{13}$$

where R, L and C are the series resistance, series inductance, shunt capacitance, all per unit length. u and i are the voltage and current.

The initial and boundary conditions are given by

$$u(z',0) = \begin{cases} 0, & 0 \le z' \le H_1 \\ u_i, & H_1 \le z' \le H_1 + H_2 \end{cases}$$
$$i(z',0) = 0, \quad u(0,t) = 0, \quad i(H_1 + H_2, t) = 0. \tag{14}$$

where H_1 is the height of the grounded channel and H_2 is the length of the in-cloud leader. The electric fields of one M-component at 30 m and 500 m were examined in *Bazelyan and Raizer* [50] (page 219, Figure 4.26).

b. Tran and Rakov [51]

Recently, as an extension of the work of *Bazelyan* [49], *Tran and Rakov* [51] developed an advanced nonlinear and nonuniform distributed circuit (RLCG) model of the lightning M-component. In contrast with *Bazelyan* [49], the shunt conductance G was taken into account in the telegrapher's equations:

$$-\frac{\partial u(z',t)}{\partial z'} = L\frac{\partial i(z',t)}{\partial t} + Ri(z',t) \tag{15}$$

$$-\frac{\partial i(z',t)}{\partial z'} = C\frac{\partial u(z',t)}{\partial t} + Gu(z',t) \tag{16}$$

with

$$L = \frac{\mu_0}{2\pi} \ln \frac{2h}{r_{core}} \tag{17}$$

$$C = \frac{2\pi\varepsilon_0}{\ln(2h / r)} \tag{18}$$

where ϵ_0 and μ_0 are the permittivity and permeability of free space, respectively, h is the height of the channel above ground level, r_{core} is the radius of the narrow channel core, and r is the outer radius of the corona sheath.

The per-unit-length series resistance R was updated after each time increment Δt as follows,

$$R(t + \Delta t) = \frac{R(t)}{1 + (\frac{R(t)i(t)}{E_{long}} - 1)(1 - e^{-\Delta t / t_g})} \tag{19}$$

where i(t), E_{long}, and τ_{g} are the instantaneous current at time t, the assumed constant longitudinal electric field, and the time constant, respectively.

The proposed M-component model consists of over 20 parameters, in which the background continuous current in their model is not constant and is accounted for in the telegrapher's equations.

The model was tested against the channel-base current and corresponding close electric fields measured for seven M-components in negative rocket-triggered lightning. Model-predicted overall power and current profiles below the cloud base were found to be consistent with the observed M-component luminosity profiles and are drastically different from the observed downward leader/upward return stroke profiles. The characteristic feature of M-components, namely the time shift between the current onset and close electric field peak, was well reproduced by their model. The predicted fields by this model were in partial agreement with experimental data (reasonable agreement was found only for 3 out of 7 measured waveforms).

4.3 Other Models and Assumptions

Mazur and Ruhnke [52] studied the physical processes of upward lightning by analyzing high-speed video images and electric field measurements. They interpreted the impulsive luminous enhancement of the lightning channel (at a relatively long time after the establishment of the upward leader) as a recoil leader intercepting the conducting channel to ground, indicating that the M-component is the result of such interception process. They proposed an

electrostatic model for the formation of the M-component process considering the concept of bidirectional leader. They argued that for the M-component, there could be no charge transfer by a downward wave inside the conducting channel to ground. In their model, after the attachment of a newly formed branch or a reactivated branch to the main channel of an upward negative lightning, the branch behaves in a manner similar to that of other upward positive leader branches. However, *Mazur and Ruhnke* [52] did not consider the transient process in the main channel.

Wang et al. [37] speculated that an M-component is composed of many waves occurring at different times and different locations. Those waves may interfere with each other in a complicated fashion. During the occurrence of an M-component, as mentioned by *Qie et al.* [15], it could be possible that many electrical breakdowns occur at different times and locations along the discharge channel. The breakdown-induced waves propagate along the same channel and superimpose on the two main waves. However, the induced waves could be weak and not distinguishable in their electric field records ([15]).

4.4 Discussion of the models

The main advantage of the guided wave model and its variations is their simplicity and straightforward implementation. Furthermore, the number of adjustable parameters in the model is limited and they can be inferred (*He et al.* [29], *Li et al.* [34]), either directly or indirectly, from experimental observations. The guided wave model is also able to reproduce reasonably well the observed electric fields.

The nonlinear models are more physics-based compared to the guided wave models. On the other hand, they are based on an important number of adjustable parameters, many of which cannot be directly inferred from experimental observations. Moreover, their field predictions appear not to be necessarily better than the guided wave models, as can be seen in *Tran and Rakov [51]*.

Finally, it is worth mentioning that all these models concern the relatively slow, millisecond scale field change. The only modeling attempt which includes the fast microsecond-scale field change is the one of *Azadifar et al.* [28], which has provided promising results. More simultaneous measurements of the current and correlated fields using either rocket-triggered lightning or instrumental towers are needed to better understand the M-component mechanism and to improve the modeling approaches.

5. Practical Aspects Related to M-components

As discussed in *Rakov et al.* [21], when *Uman et al.* [16] studied the responses of a test power distribution system to lightning strikes, they found that, in the transformer's secondary, the current pulses due to return strokes and those due to M-components had peaks of the same order of magnitude, despite the fact that in the channel-base current, the amplitudes of the M-components and return strokes differ by 1 to 2 orders of magnitude. The transformer's primary was connected to an underground cable that was connected to an overhead line subjected to direct lightning strikes.

Based on experiments at the Guangdong rocket-triggered lightning site, *Chen et al.* [17] observed the residual voltages and currents flowing in a surge protective device (SPD) connected to an overhead distribution line due to a nearby triggered lightning flash. M-components were classified into three groups in their analysis depending on the polarities of the overvoltage and the residual voltage. The total energy (129 J) of 11 M-components accounts for 34% of that from 11 return strokes flowing through the SPD (381 J). Specifically, under a given peak current, the M-component can have a greater surge energy than that of a return stroke. The continuing current on which the M-components were superimposed is believed to be an important factor in determining the voltage magnitude of line coupling in power distribution lines when a lightning flash occurs nearby.

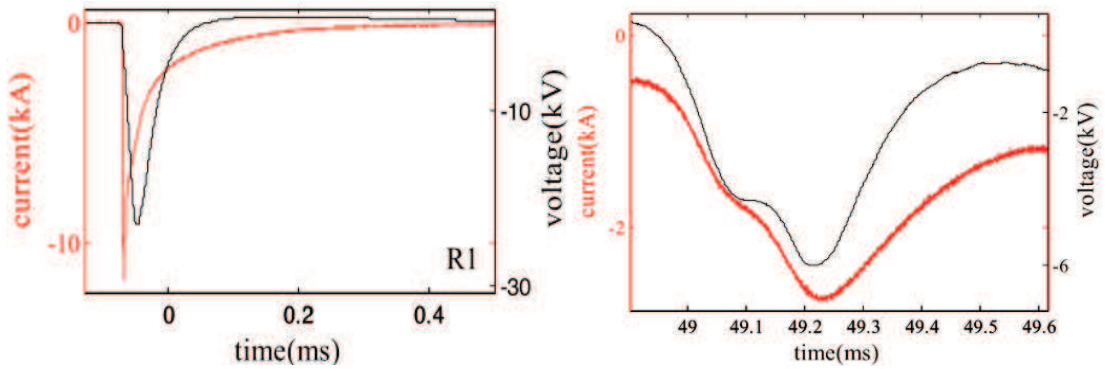

Figure 10. Current and voltage waveforms of the return stroke (left panel) and M- component (right panel) in flash T201514. Adapted from *Guo et al.* [18].

Guo et al. [18] analyzed the electrical potential and distributed current of a specifically arranged remote common grounding grid subjected to triggered lightning currents. They found that the waveforms of the measured potential and distributed current were similar to the injected current, but the common grounding grid potential may increase to as high as 5 kV, as shown in Figure 10. Even though the M-component current is small compared to that of the return stroke, it could also cause a high voltage with a maximum of −15.5 kV and an average

value of −4.6 kV to the remote grounding system.

M-components along with their continuing current transfer a significant amount of charge and may cause electrodynamic stresses and thermal effects on metallic and composite structural elements. *Smorgonskiy et al.* [65] argued that the currents used in standardized aircraft and blades of wind turbines testing should be revisited and adapted to waveforms from upward lightning flashes instead of downward lightning. The supporting evidence was as follows: (1) The charge in the standard ABCD current (<300 C) is much lower than the measured data on upward flashes obtained at the Säntis tower or in Japan; (2) currents from upward lightning exhibit a higher multiplicity (ICC pulses and return strokes) than that of downward lightning; (3) the effect of pulses superimposed on a quasi-DC current (M-components) should be studied instead of isolated pulses.

6. Discussion and Summary

We reviewed the characteristics of the current pulses and electric fields associated with the lightning M-component mode of charge transfer. We also surveyed the approaches that have been proposed to model this mode of charge transfer. Current waveforms associated with M-component-type ICC pulses in upward flashes can be distinguished from mixed mode pulses using different approaches: (i) the 10-90% risetime of measured channel-base current using as a reference value 8 μs; (ii) the time lag between the onset of the current and the electric fields, with 10 μs as a threshold value of the delay; (iii) the asymmetrical waveform coefficient (AsWc), with 0.8 as a reference value; (iv) the relative height of the junction or connection points on the grounded channel above the ground, with 1 km as a reference value.

The features of M-component electric field waveforms were summarized for three distance ranges: (i) close distance range, (ii) intermediate distance range, and (iii) far distance range. The observed millisecond-scale slow-part pulse shows a polarity reversal from an initial-negative waveform in the close range and it changes to a fully positive late-time response in the intermediate range to a bipolar waveshape in the far range. One or some microsecond-scale fast pulses (junction pulse) are observed to proceed the millisecond-scale slow part pulse at the intermediate and far distance ranges. The microsecond-scale fast pulses are dominated by unipolar pulses, although bipolar pulses with positive and negative initial polarities have also been observed.

Different approaches to model M-components were reviewed and discussed. The guided wave model and its modified versions have the merit of being conceptually simple, easy to

implement and it reproduces reasonably well the observed slow electric fields. On the other hand, physics-based nonlinear models have a large relatively number of adjustable parameters that for the most part cannot be obtained directly from experimental observations. The significance of M-components was reviewed according to practical aspects in transformers, surge protective devices (SPD), and grounding systems.

Acknowledgment

This research was supported by the Natural Science Foundation of China under Grant 51921005 and 52277160, Swiss National Science Foundation, Grant 200020_204235, and China Postdoctoral Science Foundation (2022M711759).

References

[1] Malan, D. J., and H. Collens. Progressive lightning. III. The fine structure of return lightning strokes. Proc. R. Soc. London, Ser. A, 162(909), 175–203, 1937.
[2] Malan, D. J., and B. F. J. Schonland. Progressive lightning. VII: Directly-correlated photographic and electrical studies of lightning from near thunderstorms. Proc. R. Soc. London, Ser. A, 191, 485–503, doi:10.1098/rspa.1947.0129, 1947.
[3] Rakov, V. A., & Uman, M. A. Lightning: Physics and effects. New York: Cambridge University Press, 2003.
[4] Zhou, H., Rakov, V. A., Diendorfer, G., Thottappillil, R., Pichler, H., & Mair, M. A study of different modes of charge transfer to ground in upward lightning. Journal of Atmospheric and Solar-Terrestrial Physics, 125-126, 38-49. https://doi.org/10.1016/j.jastp.2015.02.008, 2015.
[5] Thottappillil, R., Goldberg, J., Rakov, V.A., Uman, M., Fisher, R.J., and Schnetzer G.H. Properties of M components from currents measured at triggered lightning channel base. Journal of Geophysical Research: Atmospheres, 100(D12), 25711-25720, 1995.
[6] Fisher, R.J. and Schnetzer G.H. Parameters of triggered-lightning flashes in Florida and Alabama. J. Geophys. Res. Atmos., vol. 98(D12), pp. 22887-22902, 1993.
[7] Wang, D., et al., Characteristics of the initial stage of negative rocket-triggered lightning. J. Geophys. Res. Atmos., vol. 104, pp. 4213-4222, 1999.
[8] Miki, M., Rakov, V.A., Shindo, T., Diendorfer, G., Mair, M., Heidler, F., Zischank, W., Uman, M.A., Thottappillil, R., Wang, D. Initial stage in lightning initiated from tall objects and in rocket-triggered lightning. J. Geophys. Res. 110, D02109, doi: 10.1029/ 2003JD004474, 2005.
[9] Miki, M et al., Characterization of current pulses superimposed on the continuous current in upward lightning initiated from tall objects and in rocket-triggered lightning. In: Paper Presented at the 28th International Conference on Lightning Protection, Japan, 2006.
[10] Visacro, S., Araujo, L., Guimara˜es, M., and Vale M. H. M. M-component currents of first return strokes in natural negative cloud-to-ground lightning. Journal of Geophysical Research: Atmospheres, 118, 12,132–12,138, doi:10.1002/2013JD020026, 2013.
[11] Wang, C., Qie, X., Yang J. The Luminosity and Current Characteristics of M-component from Triggered-lightning in Shandong. 2010 Asia-Pacific International Symposium on Electromagnetic Compatibility, April 12 -16,2010, Beijing, China.
[12] He, L., Azadifar, M., Rachidi, F., Rubinstein, M., Rakov, V. A., Cooray, V., et al. An analysis of current and electric field pulses associated with upward negative lightning flashes initiated from the Säntis tower. J. Geophys. Res. Atmos.,123, 4045–4059, 2018.
[13] He, L., Rachidi, F., Azadifar, M., Rubinstein, M., Rakov, V. A., Cooray, V., et al. Electromagnetic fields associated with the M-component mode of charge transfer. J. Geophys. Res. Atmos., 124, 6791–6809. https://doi.org/10.1029/2018JD029998, 2019.

[14] Flache, D., Rakov, V. A., Heidler, F., Zischank, W., & Thottappillil, R. Initial-stage pulses in upward lightning: Leader/return stroke versus M-component mode of charge transfer to ground. Geophys. Res. Lett., 35, L13812, doi:10.1029/2008GL034148, 2008.
[15] Qie, X., R. Jiang, Wang, C., Yang, J., Wang, J., and Liu, D. Simultaneously measured current, luminosity, and electric field pulses in a rocket-triggered lightning flash. J. Geophys. Res. Atmos.,116, D10102, doi:10.1029/2010JD015331, 2011.
[16] Uman, M. A., Rakov, V. A., Rambo, K. J., Vaught, T.W., Fernandez, M. I., Cordier, D. J., Chandler, R. M., Bernstein, R., and Golden, C. Triggered-lightning experiments at Camp Blanding, Florida (1993-1995). Trans. IEEJ, 117(B), 446-452, 1997.
[17] Chen, S., Zhang, Y., Zhou, M., Yan, X, Lu, W., Chen, L., and Zhang, Y. Observation of residual voltage in low-voltage surge protective devices due to nearby M-components. IEEE Trans. Electromag. Compatibility, 60(3), 776–784, 2018.
[18] Guo, Z., Wu, G., Chen, S., Zhang, Y., and Wei W. Transient behavior of common grounding grids to artificially triggered lightning. IEEE Trans. Electromag. Compatibility, 61(2), 426–433, 2019.
[19] Lin, Y. T., M. A. Uman, J. A. Tiller, R. D. Brantley, W. H. Beasley, E. P. Krider, and C. D. Weidman, Characterization of lightning return stroke electric and magnetic fields from simultaneous two station measurements. J. Geophys. Res., vol. 84, pp.6307–6314, 1979.
[20] Wang, J., et al., Multiple-Station Measurements of a Return-Stroke Electric Field from Rocket-Triggered Lightning at Distances of 68–126 km. IEEE Trans. Electromagn. Compat, vol.51(2), pp. 440-448, 2019.
[21] Rakov, V. A., Crawford, D. E., Rambo, K. J., Schnetzer, G. H., Uman, M. A., & Thottappillil, R. M-component mode of charge transfer to ground in lightning discharge. J. Geophys. Res. Atmos., 106, 22817–22831. https://doi.org/10.1029/ 2000 jd000243, 2001.
[22] Zhou, H., Diendorfer, G., Thottappillil, R., Pichler, H., Mair M. Mixed mode of charge transfer to ground for initial continuous current pulses in upward lightning. In: Paper Presented at the 7th Asia-Pacific International Conference on Lightning. Tsinghua University, Chengdu, China, 2011.
[23] Paul, Ch. and Heidler, F. H. Properties of three types of M-components and ICC-pulses from currents of negative upward lightning measured at the Peissenberg Tower. IEEE Trans. Electromag. Compatibility, 60(6), pp.1-9, 2018.
[24] Paul, Ch. and Heidler, F. H. Electric field characteristics of subsequent return strokes, M-components, and ICC-pulses from negative upward lightning measured at the Peissenberg tower. IEEE Trans. Electromag. Compatibility, 61(4), pp.1138-1146, 2019.
[25] Thottappillil, R.. Rakov, V. A., and Uman, M. A. K and M changes in close lightning ground flashes in Florida. J. Geophys. Res., 95(D11), 18631–18640, 1990.
[26] Rakov, V. A., Thottappillil, R., and Uman, M. A. Electric field pulses in K and M changes of lightning ground flashes. J. Geophys. Res., 97(D9), 9935–9950, 1992.
[27] Azadifar, M., F. Rachidi, M. Rubinstein,V. A. Rakov, M. Paolone, D. Pavanello, and S. Metz. Fast initial continuous current pulses versus return stroke pulses in tower-initiated lightning. J. Geophys. Res. Atmos., 121, 6425–6434, doi:10.1002/2016JD024900, 2016.
[28] Azadifar, M., Rubinstein, M., Li, Q., Rachidi, F., & Rakov, V. A new engineering model of lightning M component that reproduces its electric field waveforms at both close and far distances. J. Geophys. Res. Atmos., 124. https://doi.org/10.1029/ 2019JD030796, 2019.
[29] He, L., et al., Modeling of Different Charge Transfer Modes in Upward Flashes Constrained by Simultaneously Measured Currents and Fields. paper presented at IEEE Inter. Symp. on EMC and APEMC, Singapore, 2018.
[30] Tran, M. D., et al., Microsecond-scale electric field pulses associated with lightning M-components, Abstract AE13B-0356, AGU, Fall Meet. 2013.
[31] Pichler, H. G., Diendorfer, G., and Mair, M. Some parameters of correlated current and radiated field pulses from lightning to the Gaisberg Tower. IEEJ Trans. Electr. Electron. Eng., 5, 8–13, 2010.
[32] Vayanganie, S., Cooray, V., Gunasekera, T.A.L.N., Nanayakkara, S., Fernando, M. Electric Field Change of M-component, paper presented at the 32th International Conference on Lightning Protection, China, 2014.
[33] Wang, J., et al., Far Electric Field Waveform in Triggered Lightning, in: Asia-Pasific Inter. Conf. on Lightning. Thailand, 2017.
[34] Li, Q., et al., Measurement and Modeling of both Distant and Close Electric Fields of an M-component in Rocket-triggered Lightning. J. Geophys. Res., 125, e2019JD032300. https://doi.org/ 10.1029/2019JD032300, 2020.

[35] Li, Q., et al., A theoretical evaluation of the instrumental decay time on electric field waveforms excited by lightning M-components. IEEE Trans. Electromag. Compatibility, 63(2), 622–626, 2021.
[36] Rakov, V. A., R. Thottappillil, M. A. Uman, and P. P. Barker. Mechanism of the lightning M-component. J. Geophys. Res., 100, 25, 701–25, 710, 1995.
[37] Wang, D., N. Takagi, and T. Watanabe. Observed characteristics of luminous variation events during the initial state of upward positive leaders. J. Atmos. Electr., 7(1), 61–68, 2007.
[38] Jiang, R., Qie, X., Yang, J., Wang, C., and Zhao, Y. Characteristics of M-component in rocket-triggered lightning and a discussion on its mechanism. Radio Sci., 48, 597–606, 2013.
[39] He, L., Azadifar, M., Li, Q., Rubinstein, M., Rakov, V.A., Mediano, A., Pavanello, D., Rachidi, F. Characteristics of Different Charge Transfer Modes in Upward Flashes Inferred from Simultaneously Measured Currents and Fields. High Voltage, Vol. 5, No. 1, pp. 30-37, 2020.
[40] Azadifar, M., Rubinstein, M., Rachidi, F., Rakov, V. A., Diendorfer, G., W. Schulz , Davide Pavanello, A Study of a Large Bipolar Lightning Event Observed at the Säntis Tower. IEEE Trans. Electromag. Compatibility, 61(3), pp.796-806, 2019.
[41] Rachidi, F., Rakov, V. A. Nucci, C. A. and Bermudez, J. L. Effect of vertically extended strike object on the distribution of current along the lightning channel. J. Geophys. Res. Atmos., 107(D23), 4699, doi: 10.1029/ 2002JD002119, 2002.
[42] Montanyà, J., van der Velde, O., Williams, E.R. The start of lightning: Evidence of bidirectional lightning initiation. Sci. Rep. 5, 15180. doi:10.1038/srep15180, 2015.
[43] Li, Q., Rachidi, F., Rubinstein, M., Wang, J., Azadifar, M., Cai, L., et al. An extension of the guided wave M-component model taking into account the presence of a tall strike object. J. Geophys. Res. Atmos., 126, e2021JD035121, https://doi.org/10.1029/2021JD035121, 2021.
[44] Li, Q., Azadifar M., Rachidi, F., Rubinstein, M., Cai, L., Zhou, M., Fan, Y., Wang J., An Extension of the Guided Wave M-Component Model Taking into Account the Presence of a Tall Strike Object, 15th International Symposium on Lightning Protection (XV SIPDA), Sao Paulo, Brazil, 30th September-4th October 2019.
[45] Li, Q., et al., A Review of the Modeling Approaches for the Lightning M-component Mode of Charge Transfer. 35th International Conference on Lightning Protection-XVI International Symposium on Lightning Protection (ICLP-SIPDA), Colombo, Sri Lanka, September 20th - 26th, 2021.
[46] Nucci, C. A. & Rachidi, F. Experimental validation of a modification to the transmission line model for LEMP calculation, 8th Symp. and Technical Exhibition on Electromagnetic Compatibility, Zurich, 1989.
[47] Rachidi, F. and Nucci, C. A. On the Master, Uman, Lin, Standler and the modified transmission line lightning return stroke current models. J. Geophys. Res. Atoms., 95(D12), 20389-20393,1990.
[48] Rachidi, F., Janischewskyj, W., Hussein, A. M., Nucci, C. A., Guerrieri, S., Kordi, B., & Chang, J. S. Current and electromagnetic field associated with lightning return strokes to tall towers. IEEE Trans. Electromag. Compatibility, 43, 356–367. https://doi.org/10.1109/ 15.942607, 2001.
[49] Bazelyan, E.M. Waves of ionization in lightning discharge. Plasma Phys. Rep. 21, 470–478, 1995.
[50] Bazelyan, E.M. and Raizer Yu. P. Lightning Physics and Lighnting Protection. Institute of Physics Publishing, 202–221, 2001.
[51] Tran, M. D., & Rakov, V. A. An advanced model of lightning M-component. J. Geophys. Res. Atmos., 124, 2296–2317. https://doi.org/ 10.1029/2018JD029604, 2019.
[52] Mazur, V., Ruhnke, L.H. Physical processes during development of upward leaders from tall structures. J. Electrostat. 69, 97–110, 2011.
[53] Jordan, D. M., V. P. Idone, R. E. Orville, V. A. Rakov, and M. A. Uman. Luminosity characteristics of lightning M components, J. Geophys .Res. Atoms., 100, 25,695–25,700, doi:10.1029/95JD01362, 1995.
[54] Kotovsky, D., M. A. Uman, R. A. Wilkes, and D. M. Jordan, High-speed video and lightning mapping array observations of in-cloud lightning leaders and an M-component to ground, J. Geophys. Res. Atmos., 124, 1496–1513, https://doi.org/10.1029/2018JD029506, 2019.
[55] Wang, X., Yuan P., Cen J., and Xue S. Correlation between the spectral features and electric field changes for natural lightning return stroke followed by continuing current with M-components, J. Geophys. Res. Atmos., 121, 8615–8624, doi:10.1002/ 2016JD025314, 2016.
[56] Yoshida, S., Biagi, C.J., Rakov, V.A., Hill, J.D., Stapleton, M. V., Jordan, D.M., Uman, M.A., Morimoto, T., Ushio, T., Kawasaki, Z.-I., Akita, M. The initial stage processes of rocket-and-wire triggered lightning as observed by VHF interferometry. J. Geophys. Res. Atmos. 117. doi:10.1029/2012JD017657, 2012.
[57] Zhang, Q., Yang, J., Liu, M., Wang, Z. Measurements and simulation of the M-component current and

simultaneous electromagnetic fields at 60 m and 550 m. Atmos. Res. 99, 537–545, 2011.
[58] Zhang, Y., Zhang, Y., Xie, M., Zheng, D., Lu, W., Chen, S., Yan, X. Characteristics and correlation of return stroke, M component and continuing current for triggered lightning. Electr. Power Syst. Res. 139, 10–15. doi:10.1016/J.EPSR.2015.11.024, 2016.
[59] Shao, X. M., et al., Radio interferometric observations of cloud-to-ground lightning phenomena in Florida. J. Geophys. Res., 100 (D2), 2749–2783, 1995.
[60] Yoshida, S., Biagi, C.J., Rakov, V.A., Hill, J.D., Stapleton, M. V., Jordan, D.M., Uman, M.A., Morimoto, T., Ushio, T., Kawasaki, Z.-I., Akita, M. The initial stage processes of rocket-and-wire triggered lightning as observed by VHF interferometry. J. Geophys. Res. Atmos. 117, D09119, doi:10.1029/2012JD017657, 2012.
[61] Jiang, R.-B., Sun, Z.-L., Wu, Z.-J. Concurrent Upward Lightning Flashes from Two Towers. Atmos. Ocean. Sci. Lett 7, 260–264. doi:10.3878/j.issn, 2014.
[62] Stolzenburg, M., et al., An M component with a concurrent dart leader traveling along different paths during a lightning flash. J. Geophys. Res. Atmos., 120, 10,267–10,284, 2015.
[63] Zhang, Y., Zhang, Y. J., Zheng, D., & Lu, W. Characteristics and discharge processes of M events with large current in triggered lightning. Radio Science, 53, 974-985. https://doi.org/10.1029/2018RS006552, 2018.
[64] Chen, M., Shen, Y., Du, Y., Dong, W. Fine spatial evolution of leaders and M-components in rocket-triggered lightning observed with a broadband interferometer. Journal of Atmospheric and Solar-Terrestrial Physics, 161, 170-184, 2017.
[65] Smorgonskiy, A., Rachidi, F., Rubinstein, M., Korovkin, N. V., and Vassilopoulos, A. P. Are standardized lightning current waveforms suitable for aircraft and wind turbine blades made of composite materials? IEEE Trans. Electromag. Compatibility, 59(4), 1320–1328, 2017.
[66] Borovsky, J. E. (1988), Lightning energetics: Estimates of energy dissipation in channels, channel radii, and channel heating risetimes. J. Geophys. Res., 103, 11,537–11,553, doi:10.1029/97JD03230.
[67] Naomi Watanabe, Amitabh Nag, Gerhard Diendorfer, Hannes Pichler,Wolfgang Schulz, Hamid K. Rassoul. Characterization of the initial stage in upward lightning at the Gaisberg Tower: 1. Current pulses. Electric Power Systems Research, 213(2022),108626, 2022.
[68] Naomi Watanabe, Amitabh Nag, Gerhard Diendorfer, Hannes Pichler,Wolfgang Schulz, Hamid K. Rassoul. Characterization of the initial stage in upward lightning at the Gaisberg Tower: 2. Electric field signatures. Electric Power Systems Research, 213(2022),108626, 2022.
[69] Li, Q., Wang, J., Cai, L., Zhou, M., Fan, Y. A discussion of the new M-component engineering model from Azadifar et al. by simultaneous measurements in rocket-triggered lightning. IEEE Letters on Electromagnetic Compatibility Practice and Applications, vol.4 (3), pp.1-5, 2022.